Assessing and enforcing single-photon returns: Poisson filtering

José Rodríguez [1], Graham Appleby [1], Toshimichi Otsubo [2],
Robert Sherwood [1], Matthew Wilkinson [1]

[1] NERC Space Geodesy Facility, UK (✉) josrod@nerc.ac.uk
[2] Hitotsubashi University, Japan

February 3, 2017

Abstract

An observation policy employed by some SLR stations is the so-called single photon ranging. This consists in controlling the intensity of the retroreflected laser pulses so that, on average, no more than a single photon per returned pulse can generate a detected photoelectron. This ensures that the optical spread distribution of the laser light, caused by the size and shape of the in-orbit retroreflector arrays, is kept constant as seen by the detection unit. Thus, accurate centre-of-mass corrections can be derived for stations employing this mode of operation. The criteria used to control the intensity of returned pulses consists typically in setting a sufficiently low target detection rate (e.g. 10%). In the past, the low, but greater than zero probability of detecting multi-photon events at these modest rates was reasonably considered to have little impact on the quality of the observations. However, in the era of mm-level geodesy, every possible effect should be taken into account, and previous assumptions revisited. Here we add to the evidence showing that multi-photon detections, even at controlled, single-photon rates do occur and have a small, but quantifiable impact on the ranging measurements. We present a post-processing filter based on Poisson statistics that in our tests proved effective to remove this effect, bound by our results to less than 1 mm for LAGEOS/LARES and less than 2 mm for Ajisai. We discuss how a combination of the real-time energy control system plus a post-processing step makes of single-photon ranging an observation policy that enables sub-mm accuracy.

1 Introduction

The satellite laser ranging tracking stations that comprise the ground network of the ILRS do not employ, with the exception of certain subnetworks (NASA, Russian stations), a standardised set of technologies. System features such as telescope type, size and mount; laser equipment; detection hardware; timing devices; and computer control, vary wildly from one station to the next. The cause for this heterogeneous choice of hardware solutions derives from the manner in which the network has been deployed and expanded, whereby research teams from multiple institutions in several countries developed and perfected their own systems. Thus, with the exceptions mentioned above, a majority of laser stations that have ever contributed observations to the ILRS network are to a large extent unique systems. From the operational point of view, it is therefore not surprising to find that different observation policies are in place across the network, as different hardware choices enable, limit or dictate the mode of operation.

The observation policy or mode of operation of a laser station refers to the intensity of the returned laser pulses which are to be detected. Stations performing ranging measurements on the basis of the detection of laser pulses containing several photons are referred to as multi-photon systems. Most legacy laser ranging stations built before the widespread availability of very high repetition rate lasers (KHz rates) aimed to operate at the multi-photon regime. An alternative mode of operation is the

Table 1 – Typical observation policies of SLR stations

mode of operation	number of photons in returned pulses	typical reference point	typical hardware requirements
multi-photon	tens	leading-edge	high energy per shot, reasonable size primary mirror
few photon	?	?	N/A
single photon	< 1	centroid	mechanism to control return energy

so-called single photon ranging, whereby the intensity of the returned pulses is limited so that no more than an individual photon should generate a detected photoelectron. This technique was pioneered in the early 1990s at the Herstmonceux station in the United Kingdom, in close connection with the development and availability of a detection technology alternative to photomultiplier tubes (PMTs): the avalanche photodiodes. With very fast rise times and high light sensitivity, the development of single photon avalanche photodiodes (SPADs), carried out and adopted predominantly in Europe, provided an attractive alternative to PMTs. As various groups gained experience with this kind of detectors, it became obvious that there were features in the ranging data that were not apparently present when employing PMT detectors. It was understood that the intensity of the returned pulses is a critical variable that affects the timing of the observations (i.e. the ranges themselves), and several solutions and recommendations were pursued and made. Of major significance was the improved knowledge, backed by newly obtained empirical data, of the impact the size and shape of laser retroreflector arrays have on the ranging measurements. Previously assumed to be of little importance in practical terms, it was demonstrated that different systems respond in different ways to the pulses returned from different satellite targets, which called for the development of models to account for these effects to compute system-specific centre of mass correction values. In this paper we review briefly the concept of single photon ranging, we quantify the extent to which current practices may negatively impact the range observations, and provide a post-processing filtering method to detect and edit out the presence of detections that could potentially compromise the accuracy of the data.

2 Single photon ranging

In order to ensure maximum consistency in the laser ranging observations, it is recommended to limit in some way the variations in intensity of the returned pulses. For this purpose, many stations control their detection rates to some extent, regardless of the mode of operation followed (see table 1). In single photon mode, controlling the return rate is the only method to ensure operation at intensities of one photon or fewer (on average) per received pulse. Having the means to limit and control the return rate in real time involves some modest extra complexity in the form of a few additional hardware components plus the software required to drive them. Nonetheless, the motivations to operate at the single photon level are manifold:

- total absence of detector time-walk
- absence of satellite signature intensity dependent effects
- possibility to compute accurate CoM corrections
- ranging data to flat GNSS arrays theoretically not affected by incidence angle
- single mode of operation during calibration, standard ranging and data reduction, regardless of satellite height and elevation, laser retroreflector array cross-section, weather conditions, and the presence/absence of day time filters

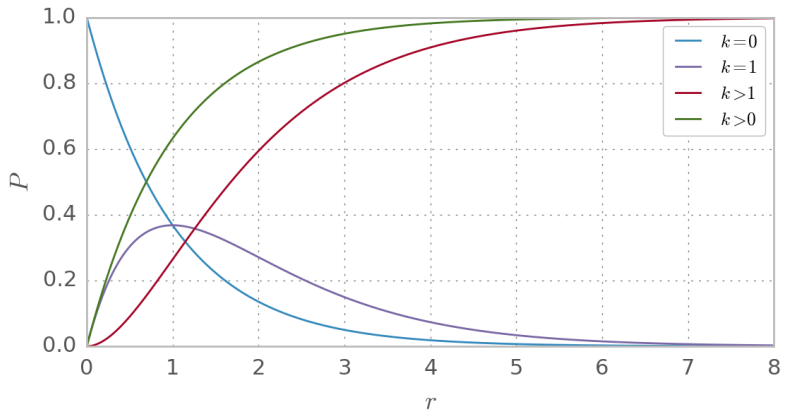

Figure 1 – Poisson probability distributions $P(k,r)$ for various k events and average rates, r, up to eight. $P(k>0,r)$ is the detection probability, without discriminating between the number of events, whereas $P(k>1,r)$ is the probability of obtaining multiphoton events.

All these items have their origin in the low intensity of the return pulses and the high consistency achieved when operating in this mode. As only one photon at most on average triggers a successful detection, there should be no variations in the returned intensity that could cause detector time-walk effects, or skew the detection point towards the leading edge of the returned pulses. Furthermore, laser photons reflected off any point of the in-orbit laser retroreflector arrays are detected with a relative probability that only depends on the geometrical distribution of the individual corner cubes (position and orientation). Therefore the problem of computing CoM values for stations operating at single photon mode becomes more tractable and is subject to fewer assumptions than in the case of other observation policies.

It must be noted that other modes of operation, choice of hardware devices, and data reduction schemes offer their own solutions to the issues mentioned above, with several world class stations demonstrating their successful implementation. However the future shape of the network will consist almost exclusively of stations operating in the single photon mode, both because of its own merits, and because the most attractive hardware systems for modern stations (very high repetition and low energy laser systems, modest size telescopes) dictate, in practice, this observation policy.

2.1 Measuring and controlling the return rate

Poisson statistics. Normally there are no means available to perform a direct measurement of the energy of the detected pulses. Therefore, it must be estimated in an indirect way, through the rate of detections. Since both photon arrivals and the photoelectron conversion at the photocathode of the detector follow Poisson statistics [1] , a simple count of the successful detections for a period of time provides an estimation of the Poisson intensity. The probability distribution for a Poisson process is given by:

$$P(k,r) = \frac{r^k e^{-r}}{k!} \tag{1}$$

[1] Photon detection is a Bernouilli process (only two possible outcomes: success or fail) whose probability is given by the binomial distribution, which in turn converges to the Poisson distribution for a large number of trials and/or low probability values.

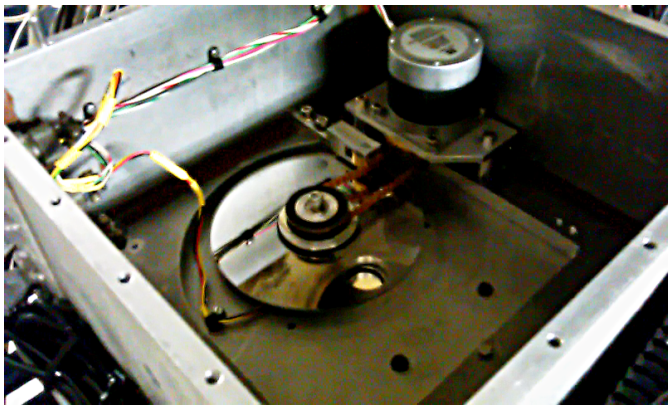

Figure 2 – Attenuation control device installed at Herstmonceux station. A neutral density wheel is positioned slightly off-axis relative to the incoming beam of light at the back of the receiver. A stepper motor rotates the wheel as required in order to change the filter transmission.

where k is the number of events (successes) and r is the Poisson rate or intensity. The probability distribution for some interesting values of k are given below:

$$P(k=0,r) = e^{-r} \tag{2}$$
$$P(k=1,r) = re^{-r} \tag{3}$$
$$P(k>0,r) = 1 - P(0,r) = 1 - e^{-r} \tag{4}$$
$$P(k>1,r) = 1 - P(0,r) - P(1,r) = 1 - (1+r)e^{-r} \tag{5}$$

These distributions give the probability of obtaining 0, 1, *any*, and *multiphoton* detections, respectively. Figure 1 displays the distributions above, where it can be noted that the probability of obtaining multiple events is significant even below unity rate levels. The average rate is obtained counting the number of detections over some time interval, which renders the maximum likelihood estimator for r. In order to avoid underestimating the average rate, noise events should be taken into account in the computation, although the impact is low except for very high noise rates. We must stress that in the context of laser ranging, the rates refer to *detection* rates, that is, *photoelectrons* generated at the photocathode, rather than *photons* at the entrance of the telescope. If one were interested in working with units of photons or light flux in connection with detection probabilities, the quantum efficiency of the detector plus any other optical losses would have to be taken into account.

Instrumentation. Estimating the detection rates is, as detailed above, a trivial counting exercise. In order to limit and control the rate of detections, this information is used in conjunction with some hardware means to vary the detection probability. Some possibilities to achieve this include:

- variable neutral density filter in the receiver path
- variable neutral density filter in the transmitter path
- divergence control
- pointing offsets
- laser energy control

Of this list the first three options appear equally optimal, whereas the last two appear difficult to implement, either operationally (pointing offsets), or from the engineering point of view (control of laser energy). At the SLR station in Herstmonceux a variable neutral density filter wheel is installed in the receiver path, controlled by a stepper motor that can thus swiftly attenuate the incoming photon

flux in a continuous manner (see figure 2). The detection rate is continuously estimated in real time, and a simple software control scheme drives the actuator to keep the rates sufficiently low to ensure a very low probability of obtaining multiple photon events. In practise the detection rate is kept below 12% when operating the 1 KHz firing rate laser ($P(k > 1, 0.12) = 0.66\%$). Variable divergence control is also implemented at this station, although its primary use is to widen the beam radius for low Earth orbiting satellites in order to optimise acquisition times.

Evidence of multiphoton events. The underlying assumption underpinning the estimation and control of detection rates as detailed here is that the conditions under which the observations are collected are adequately described by a homogeneous Poisson distribution. In other words, that the Poisson rate is fairly constant over sufficiently long periods of time. Otherwise, the estimation of a constant, average rate by a simple count is not valid, and consequently it is not possible to control the detection rates. The question of whether constant rates can be assumed under all practical circumstances had not been satisfactorily answered in the past. Nonetheless, the success achieved at Herstmonceux station with this mode of operation shows that deviations from the ideal homogeneous Poisson process must have a rather limited effect. However, recently Eckl and Schreiber (2015) demonstrated that with their system (Wettzell, Germany), even at the low, controlled rates typical of single photon operation, multiple events are registered which have the potential to skew the ranging observations. These results were obtained by measuring directly the energy of the incoming pulses with a MCP detector, and were replicated for various satellites. The authors concluded that under real world conditions, the presence of clouds, pointing errors, noise events and uncertainties in the rate estimation mean that purely single photon data can not be obtained.

3 Poisson filtering

Real time detection rate estimation under normal tracking conditions is subject to practical difficulties that compromise its accuracy, and therefore the performance of the control scheme. For this reason, a post-processing step is recommended in order to identify and edit out observations whose detection rate may be higher than some acceptable threshold (e.g. 10%). A straightforward counting method whereby detection rates are computed offline has been in place at Herstmonceux station since the beginning of its operations at single photon, ensuring that the normal point and full rate data submitted complies with the observation policy as much as possible. The question is whether, in light of Eckl and Schreiber (2015) results, this is sufficient. The weak point of any scheme that relies on binning the data at equally spaced intervals to compute the detection rate is that the result is an average per bin. If the data contain intensity variations with temporal characteristics that can not be captured by the bin size employed, there may be situations where while the computed average rate may not exceed the desired maximum threshold, high rate observations fail to be rejected. Of course, reducing the bin size is an obvious workaround, although it is not obvious what an optimal criteria to select it would be, and in any case because of the bin boundaries some averaging effect would still occur.

Our new filtering scheme relies in measuring the interarrival times t_k between each satellite detection i and the next $i + k$ ones, with $k = 1, 2, ...n$; limiting n to 13 from practical experience with our 1 KHz rate ranging data. From Poisson statistics we can then compute, for an assumed target return rate, the probability of obtaining k events in each time interval t_k, and use these values as the basis for data acceptance by setting a suitable minimum probability threshold. This filter has the highest possible granularity (it can reject two consecutive detections if their probability is too low), and it is continuous, as the test is performed on every detection in relation to its previous and next n neighbours. In practice, we first compute and store the minimum time windows T^k_{min} at which k events can be observed with a probability higher than a minimum threshold; the t_k timings are then compared to their respective T^K_{min} values and observations rejected if $t_k < T^k_{min}$.

The Poisson probability distributions displayed in figure 3 illustrate how we can compute the

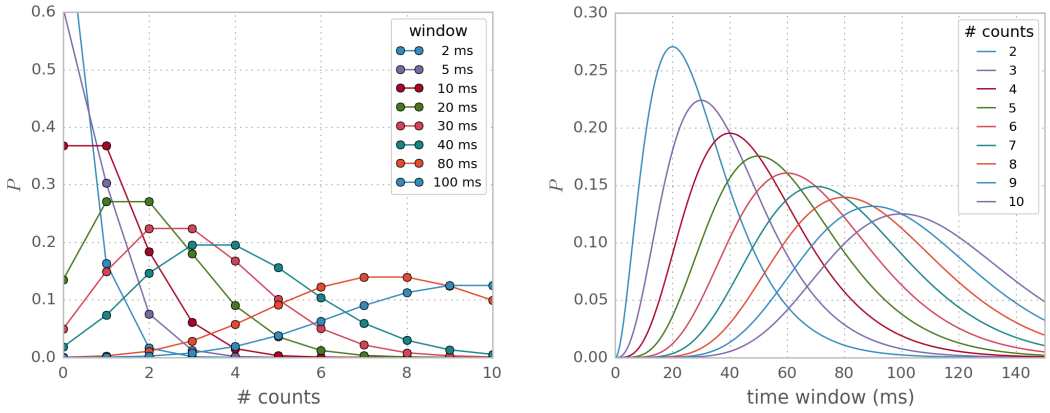

(a) **(b)**

Figure 3 – Probabilities of observing k events at 10% detection rate and 1 KHz firing rate for different time intervals. Both plots display essentially the same information, with the series on the left corresponding to time windows and to number of counts on the right.

required interarrival times for the filtering scheme. Instead of estimating the detection rate at fixed bin intervals, a maximum accepted target rate is assumed, e.g. 10%. Introducing in expression 1 the detection rate computed from the firing rate and the target detection rate for different time windows we compute the probability of obtaining k events. For instance, at 1 KHz firing rate and 10% target detection rate, the expected average rate in 100 ms is 10 events; with this rate we obtain the probability of observing $k = 2,3,...n$ events, as shown in figure 3a. A more convenient way to display this is to compute the probability distributions $P(k,r)$ at every possible interval, as in figure 3b. Setting a minimum acceptable probability threshold we can ascertain from the plot the shortest time interval at which each group of k counts is expected. For instance, the intersection of the horizontal line $P_{min} = 0.1$ with the curve for $k = 4$, indicates that the $T_{min}^{k=4}$ value is approximately 20 ms (at 1 KHz and 10% rate). The required intervals can be easily computed numerically for later use in the actual data filtering stage.

An adequate implementation of the filter involves: i) precomputing the T_{min}^{k} values for $k = 2,3,...n$ for a target maximum rate; ii) looping over all the observations, comparing the interarrival times t_k to the minimum accepted intervals, rejecting if $t_k < T_{min}^{k}$; iii) store the timing of the current observation in a ring buffer for use in the next n loop iterations. Note that in practise we employ the interarrival times of each observation in relation to the n previous ones.

3.1 Results

We tested the performance of this filtering strategy on the full rate data collected at Herstmonceux with the 1 KHz laser system for various satellites. An example of the action of the filter is shown in figure 4, corresponding to a LARES pass. The top subplot of the figure displays the original ranging residuals, with individual tracks of single retroreflectors visible. Some amount of banding is also apparent; these are short bursts of detections with a rate evidently higher than the rest of the data. These regions are correctly identified and rejected by the filter, as seen in the middle panel of figure 4. The remaining data (bottom subplot) is exempt of any such banding and presents a more homogeneous data density throughout the pass. It is remarkable that despite rejecting almost 50% of the data, the remaining residuals do not appear to contain any obvious gaps, indicating an excellent filter granularity. Evidence

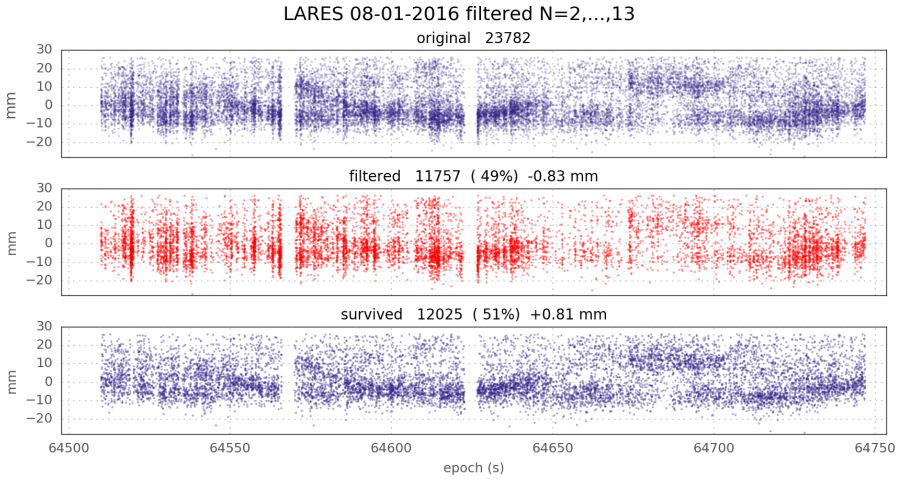

Figure 4 – Observation residuals of a LARES pass. Top: original data; middle: filtered out (rejected) observations; bottom: remaining (survived) data. The displacement of the mean in the filtered and remaining data is 0.8 mm in opposite directions relative to the original data. All groups of k events with $k = 2, ...13$ have been filtered, resulting in an excessive rejection of about 50% of the data.

that the filter is rejecting events that are statistically more likely to contain multiphoton data is provided by the displacement of the mean of the residuals relative to the original data. The rejected data (middle subplot in figure 4) is displaced towards shorter ranges, the direction expected for high intensity detections, by 0.8 mm. The remaining data presents the opposite behaviour, with its mean of residuals displaced about 0.8 mm towads longer ranges. However, rejecting almost half of the original data seems excessive, and it may indicate that the filter settings are not properly tuned. If the target detection rate is set much lower than the actual average at which the original data was collected, or the minimum accepted probability threshold is too low, the filter will (correctly) flag many events as having a low expectation value, resulting in their rejection.

Tuning. An analysis of the filter behaviour in terms of the displacement in the mean of residuals for each group of k events offers the opportunity for an optimisation strategy. The displacement in the mean of residuals for the data shown in figure 4 is displayed in figure 5. Clearly, the displacement in the mean for each group is not constant, which simply indicates that the distribution of bursts of higher rate data is not flat in terms of their duration. Thus, we could reject only those groups of k events that show the highest mean displacement, and accept the remaining ones. This is best done on the basis of displacement of the mean of residuals per detection event (see right subplot in figure 5) to ensure the highest filter efficiency (rejection of the groups with highest displacement while preserving the maximum amount of data). In this example, rejecting only two groups of events according to the absolute magnitude of their displacement of the mean would lead to the rejection of groups $k = 10$ and $k = 11$. Taking the displacement of the mean per event as our selection criteria leads to the rejection of groups $k = 3$ and $k = 4$.

The result of constraining the filter to only rejecting two groups of events is shown in figure 6. In this case only 27% of the data was rejected, with the mean of rejected residuals displaced by 1.5 mm relative to the original data. The mean of the remaining observations if offset 0.56 mm towards longer ranges. Limiting the action of the filter to groups of events with the highest displacement in the mean appears to be a satisfactory strategy to avoid excessive filtering while rejecting high rate data. A notable example of the effectiveness of this optimisation is shown in the appendix for an Ajisai pass.

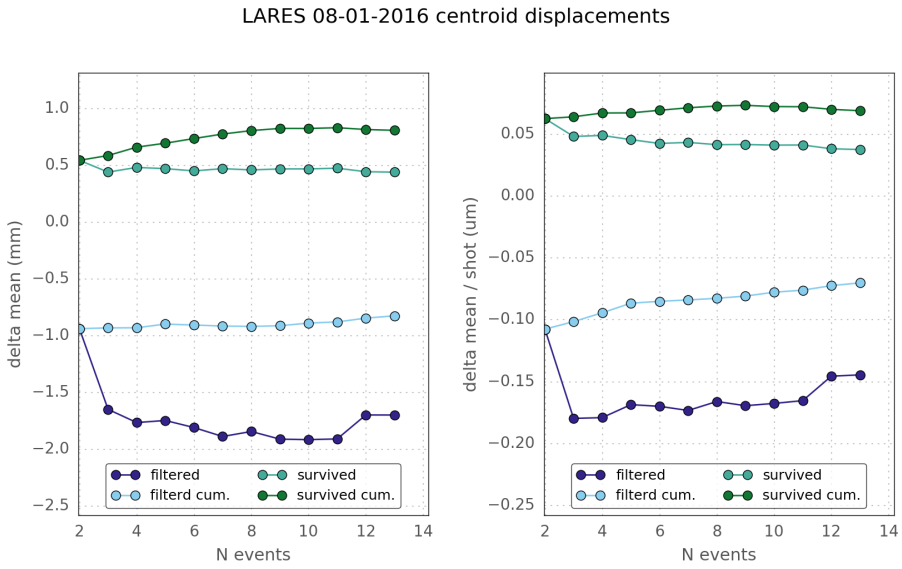

Figure 5 – Displacement of the mean of residuals for each group of k events of the data shown in figure 4. Mean displacement is given for the filtered (rejected) and remaining (survived) observations, both in individual and cumulative terms. Left: total mean displacements per group of events, in mm. Right: mean displacements per observation, in μm/shot.

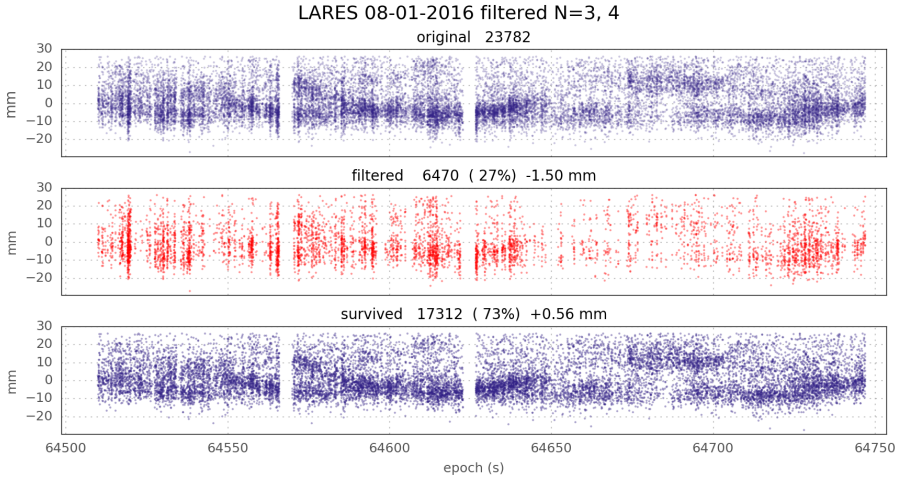

Figure 6 – Filter performance rejecting only two groups of events, chosen according to the magnitude of the displacements of their means per event. The number of observations kept is much higher than in the case of applying the filter naively.

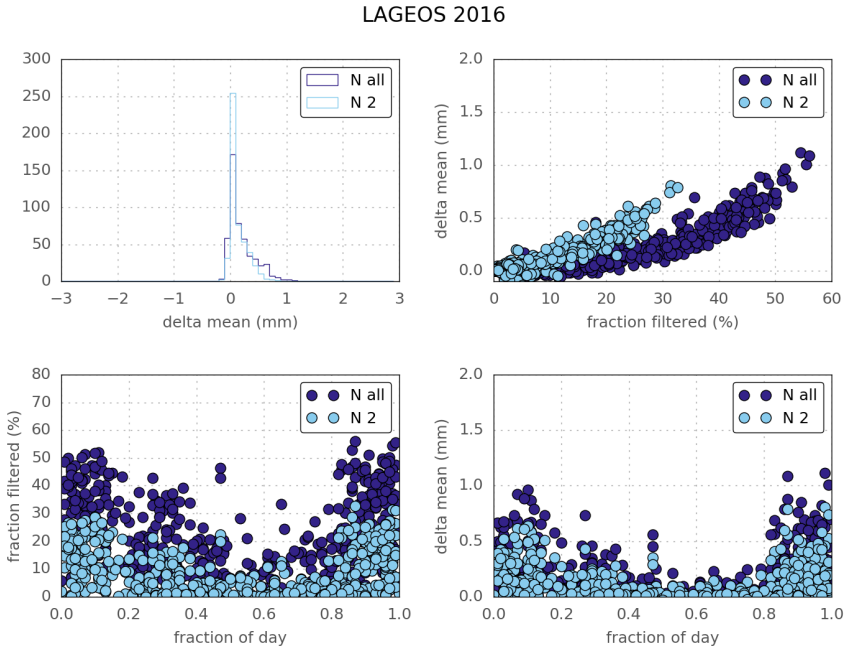

Figure 7 – Filtering of LAGEOS 2016 full rate data. The dark traces correspond to the application of the filter rejecting all groups of events that fail the filter criteria. In lighter colour is shown the effect of applying the filter constraining its action to the two groups of events with maximum displacement of the mean per event.

Analysis of annual data sets. We investigated the effect of applying our Poisson filtering scheme to all the full rate data files collected at Herstmonceux during one year for various satellites. Here we limit our exposition to a summary of the results obtained for LAGEOS data during 2016, although we include the equivalent plots obtained for Ajisai in the appendix.

The distribution of the displacement of the mean of residuals for the 2016 data after applying our filter is shown in figure 7. The first item to note is the distribution of the displacement of the means of residuals after applying the filter. The mode of this distribution is very close to 0, but it has a tail that extends to 1 mm in the positive direction, i.e. the average offset in the ranges of the data attributable to the presence of observations with a higher return rate than strictly single photon is less than 0.5 mm. Next, the effect of constraining the action of our filter to only two groups of events, as discussed in the previous section, is clearly seen in the top right subplot of figure 7: for an almost identical displacement of the mean (i.e. filter effectiveness) the fraction of observations filtered is more than halved.

Interestingly, there is a clear correlation between the time of the observations and the amount of data rejected by the filter (or the displacement of the means). It is found that at night time it is more likely that the filter finds data suspected to contain high return rate observations. The explanation is that the detection rate at night tends to be higher, as the narrow band spectral filter (the physical filter employed to reduce background noise during daytime operations) is removed when its use is not required. In this conditions, the efficiency of the receiver system is increased and the real time return rate estimation and control is more often challenged to keep single photon operations. Interestingly, this correlation with time of the day is not seen for targets with very strong reflections such as Ajisai, as the return rate is quite high regardless of whether the daytime spectral filter is employed.

4 Conclusions

We have presented a filtering scheme based on Poisson statistics that aims to detect and reject ranging data with a high probability of containing observations whose return rate is higher than expected for strictly single photon operations. The filter can be used not only for rejection purposes, but as an assessment of the presence and quantitfication of multiphoton events, which may inform system developers wishing to adopt a single photon observation policy to optimise their real time return rate control schemes. It is found that even after applying an average return rate estimation method on the binned full rate data the presence of multiphoton events can not be discarded. The maximum impact on the ranging measurements is, however, limited to 1 mm at most for LAGEOS and 2 mm for Ajisai, with an average at the sub-mm level.

Multiphoton events when operating at single photon mode have their origin in practical difficulties encountered under real world conditions. In our experience, the major source of multiphoton events are pointing variations when ranging with a low beam divergence, which result in return rate variations and the presence of bursts of high intensity data. We have determined that the use of higher beam divergences minimises this effect, and we are studying the most convenient settings to keep the most stable detection rates during real time operations.

At the post-processing stage, the application of the filter scheme described here is a useful method to ensure the distribution of full rate observations is as absent as possible from multiphoton events, and that therefore the normal point data is unbiased. The combination of these measures, *viz.* real time control, optimisation of system ranging settings, and use of a post-processing filter, at KHz firing rates, ensure that the contribution to the total error budget attributable to the observing policy itself is limited to a few tenths of a mm at most.

References

Eckl, J. J., and U. Schreiber. 2015. Single photon tracking under difficult condition. In *2015 ILRS Technical Workshop. Network Performance and Future Expectations for ILRS Support of GNSS, Time Transfer and Space Debris Tracking*. Matera, Italy.

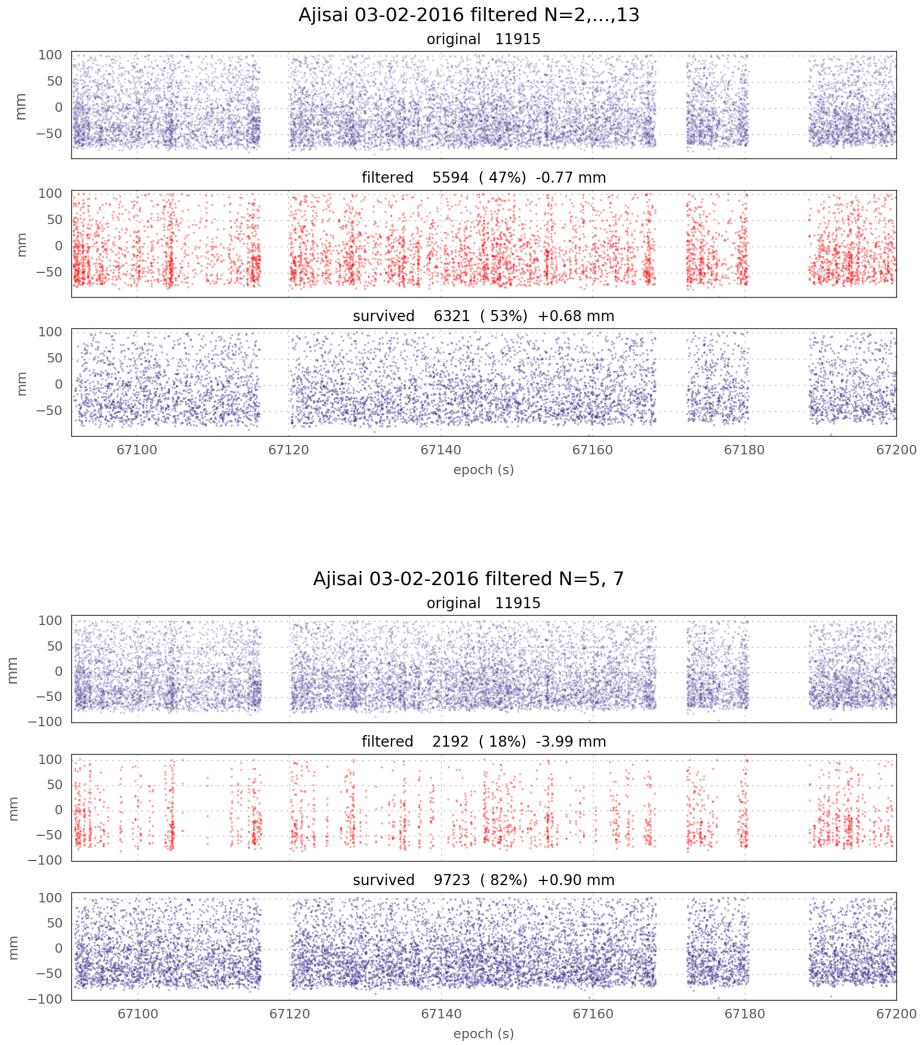

Figure 8 – Filter performance for an Ajisai pass. Top: rejecting all groups of k events that fail the rejection criteria. Bottom: rejecting only the two groups of events with the highest displacement in the mean ($k = 5$ and $k = 7$). The second option not only leads to a much smaller fraction of the data being rejected, but also affords a greater correction in the mean of the remaining residuals. It is remarkable that the filter is able to reject very short data bursts whose presence is not evident by visual inspection.

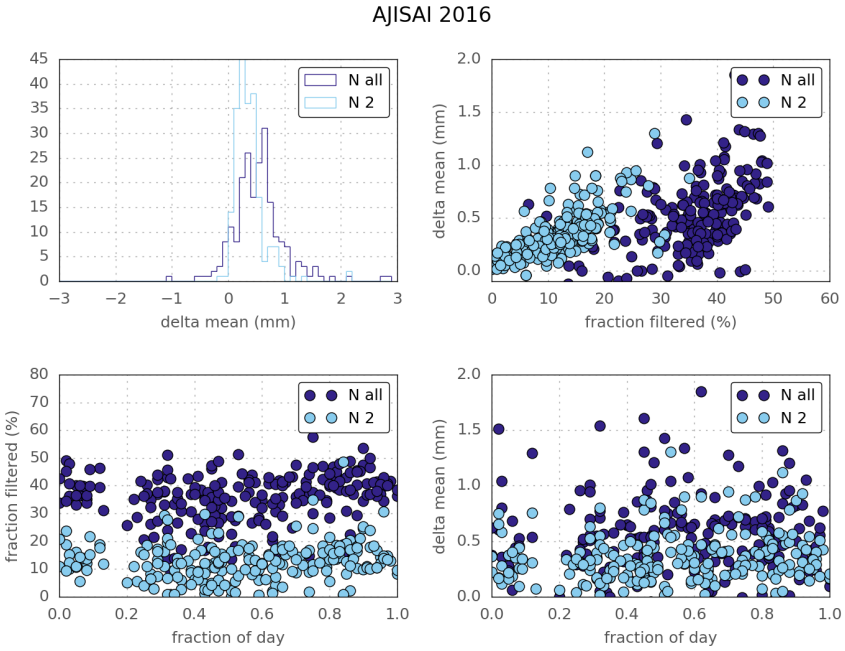

Figure 9 – Filtering of Ajisai 2016 full rate data. The dark traces correspond to the application of the filter rejecting all groups of events that fail the filter criteria. In lighter colour is shown the effect of applying the filter constraining its action to the two groups of events with maximum displacement of the mean per event.